Thermal stability of barium-doped iron oxides with spinel structure

Ch. Sarda * and A. Rousset

Laboratoire de Chimie des Materiaux Inorganiques, URA CNRS 1311, Université Paul Sabatier-Toulouse III, 118 Rte. de Narbonne, 31062 Toulouse Cedex (France)

(Received 5 November 1992)

Abstract

Previous experiments have demonstrated the influence of the size and surface area of particles of iron oxides with spinel structure on the oxidation ($Fe_3O_4 \rightarrow \gamma\text{-}Fe_2O_3$) and transformation ($\gamma\text{-}Fe_2O_3 \rightarrow \alpha\text{-}Fe_2O_3$) enthalpies and temperatures. In the present paper, the modification of these processes by a Ba doping is studied. This ion does not form a solid solution with the iron cations but is located in the superficial layers of the particles.

The oxidation enthalpy of magnetite, linked to the cationic migration of ferrous ions in the spinel structure, is not modified as such. However, the temperature at which this phenomenon appears increases due to the presence of a diffusion barrier at the surface of the particles.

The stability of the lacunar phase $\gamma\text{-}Fe_2O_3$ is also increased by Ba doping. The progressive recoverage of the particle by a Ba-rich phase prevents the generation and sliding of dislocations.

INTRODUCTION

Because of the great interest shown in the properties and applications of pure, substituted, and doped spinel ferrites and related defect spinel systems [1–3], several authors have studied in detail the kinetics, mechanisms and thermodynamics of the two reactions:
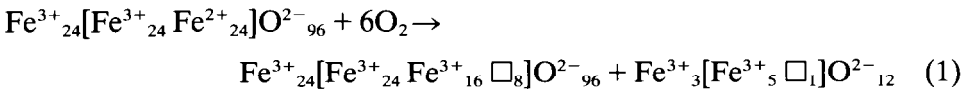
(i) The oxidation $Fe_3O_4 \rightarrow \gamma\text{-}Fe_2O_3$, corresponding to the oxidation of ferrous ions, with no change in the spinel structure;

(ii) The topotactic transformation $\gamma\text{-}Fe_2O_3 \rightarrow \alpha\text{-}Fe_2O_3$, which represents the limit of stability of the lacunar phase.

For the oxidation of magnetitie into maghemite, the model explaining the mechanism is based on the diffusion of Fe^{2+} ions from the bulk to the surface, where they form new layers with a spinel structure, in combination with O_2. The migration of a portion of the Fe ions creates vacancies in the bulk [4, 5].

This process, summarized in eqn. (1), shows that migration involves only

---

* Corresponding author.

8 ferrous ions, the other 16 ions being oxidized in situ

$$Fe^{3+}{}_{24}[Fe^{3+}{}_{24} Fe^{2+}{}_{24}]O^{2-}{}_{96} + 6O_2 \rightarrow$$
$$Fe^{3+}{}_{24}[Fe^{3+}{}_{24} Fe^{3+}{}_{16} \square_8]O^{2-}{}_{96} + Fe^{3+}{}_{3}[Fe^{3+}{}_{5} \square_1]O^{2-}{}_{12} \quad (1)$$

The cations in the brackets are in the octahedral sites; the others are in the tetrahedral sites.

The transformation γ-$Fe_2O_3 \rightarrow \alpha$-$Fe_2O_3$, where the lattice rearrangements take place by relative sliding of the layers along directions parallel to the (111) planes, has a different mechanism. The dislocations needed are generated between the oxygen planes which sandwich the mixed trigonal lattice, because the number of Fe–O bonds to be broken is lower (one for each tetrahedral site and three for each octahedral site) than in the kagomé lattice [6].

The temperatures of these exothermic phenomena, studied by several authors, depend on morphological (sizes and shape of the particles) and chemical (purity and ion substitution) factors.

Egger and Feitknecht [7] have shown that particle size controls the reaction rate and the phase (γ- or α-Fe_2O_3) obtained from the oxidation process; smaller particle sizes lead to the lacunar spinel structure alone. Gallagher et al. [4], Colombo et al. [8] and Gillot et al. [3] have confirmed this result and have determined the maximum size to conserve the spinel structure.

For the allotropic transformation of Fe_2O_3, Bando et al. [9] have shown that the temperature of the phenomena decrease as particle size increases. Dupré [10] obtained the same results with cobalt-doped particles, and elaborated on the influence of the morphological characteristics, confirming Imaoka's previous results [11].

The influence of the substitution of ferrous or ferric ions on thermal properties has been studied more recently. Generally speaking, substitution by mono- or divalent ions increases the stability of the spinel phases (Fe_3O_4, γ-Fe_2O_3). For example, introduction of 10 wt.% of cobalt or 15 wt.% of zinc increases the oxidation temperature by about a hundred degrees. Zinc ion also allows an increase in the temperature of the allotropic transformation [10]. This can be explained by the reduction in the number of lacunar sites (and an increase in the diffusion factor) when divalent ions are employed [12], but substitutions by trivalent ions (without variation in the number of vacancies) [12, 13] or tetravalent ions (an increase in the number of vacancies) [14] lead to the same results.

The surface dopings of magnetite particles by boron or cobalt ions [15] involve at least an increase in the temperature of both thermal phenomena. The energies linked to these phenomena and their variations have not been the subject of so much research.

For the oxidation of magnetite, some values may be obtained, generally

for the total reaction of Fe_3O_4 into α-Fe_2O_3, including oxidation and transformation [16, 17]. In previous work [18], we determined the energy for the oxidation $Fe_3O_4 \rightarrow \gamma$-$Fe_2O_3$, and pointed out the influence of the surface area and state of division of the particles.

The enthalpy of reaction for the allotropic transformation was first determined by Ferrier [19]. The influence of grinding and of surface area were subsequently studied by Imai and Senna [20] and by Rousset et al. [21].

In the present paper, the variation in the temperature and energy of the two reactions described for particles of barium-doped iron oxide are studied. The presence of the alkaline-earth ion is indeed very interesting because of its ionic radius; it is expected to be out of the spinel structure of magnetite or maghemite and, in this way, it does not modify the magnetic properties of these compounds which are of great interest for high-density magnetic recording [22]. For this application, it is very important to obtain a high thermal stability of the pigments.

SAMPLE PREPARATION AND CHARACTERIZATION

The samples were prepared from ferrous oxalic precursors. Precipitation takes place in an alcohol solution to obtain sub-micronic particles. The products obtained correspond to $FeC_2O_4 \cdot 2H_2O$, and the addition of barium salt leads to the formation of a second phase containing only Ba ions, $BaC_2O_4 \cdot 0.5H_2O$. The presence of this compound was identified by X-ray diffraction when barium ions are present in sufficiently large quantities (about 2 wt.%).

The iron oxide particles with spinel structure are generated in a sequence of successive thermal treatments:

(i)   Oxalate decomposition in air (about 400–700°C)
(ii) Reduction under $N_2(90\%)/H_2(10\%)$ atmosphere (300–400°C)
(iii) Annealing under N_2 atmosphere at about 500°C to improve particle crystallization

The product obtained was Fe_3O_4, as determined by X-ray diffraction. To obtain γ-Fe_2O_3, it was necessary to oxidize magnetite by thermal treatment at about 250°C in air.

Any Ba-containing phase was identified by X-ray diffraction, and infrared spectroscopic analysis was used to detect the presence of barium hydroxide, $Ba(OH)_2 \cdot 8H_2O$, or barium ferrate, $BaFe_2O_4$ [22].

Analysis of the X-ray diffraction patterns shows that the a lattice parameter, either for Fe_3O_4 or γ-Fe_2O_3, is not sensitive to the amount of barium included in the structure (Table 1), despite the relatively larger

TABLE 1

The size of the *a* lattice parameters of Fe_3O_4 and γ-Fe_2O_3 with different amounts of barium in their structures

Barium in wt.%	Lattice constant of Fe_3O_4 in nm	Lattice constant of γ-Fe_2O_3 in nm
0	0.8396	0.8345
0.3	0.8396	0.8346
0.45	0.8396	0.8345
0.58	0.8396	0.8345
0.74	0.8394	0.8346
1.54	0.8396	0.8344

ionic radius of the Ba ion (0.134 nm) compared with the size of the octahedral and tetrahedral sites. The substitution of ferrous (0.078 nm) or ferric (0.064 nm) ions by Ba ions would invariably lead to a very high distortion of the individual lattice of these spinel structures.

More extensive analysis by secondary-ion mass spectroscopy enables the location of the barium ions to be determined. The concentration profiles of the Ba^+ ions with respect to the depth of the analysis for several samples show that these ions are highly concentrated in the first layers (about 5 nm) on the particle surface (Fig. 1). Simultaneously, the Fe ion concentration decreases from the bulk towards the surface (Fig. 2).

It can then be inferred that the barium ions are only present near the surface of the particles. These particles, with a spinel structure in the core and a second outer phase containing Ba ions at the surface, are those that are obtained.
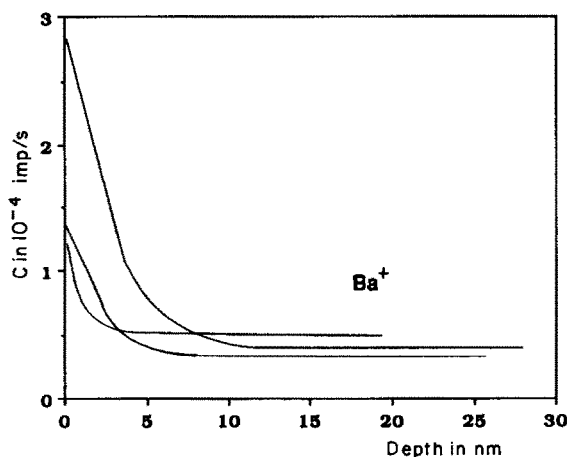

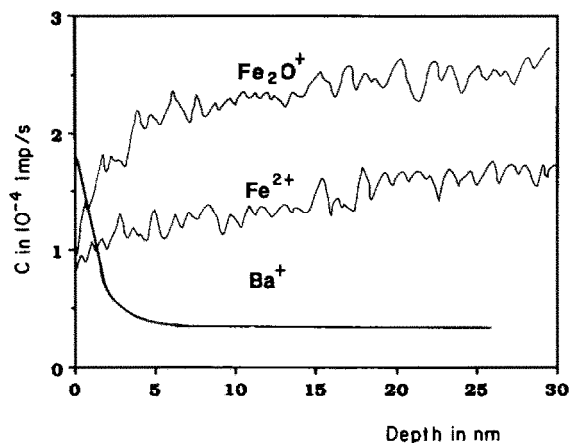Fig. 1. SIMS concentration profiles of Ba^+ ions as a function of the depth of analysis.

Fig. 2. SIMS concentration profiles of Ba^+, Fe^{2+}, and Fe_2O^+ ions as a function of the depth of analysis.

To avoid variations due to the influence of particle size, the conditions of the thermal treatments were chosen to obtain mean particle sizes in the range 40–50 nm, as measured by Scherrer's method from the X-ray diffraction patterns (Table 2).

The amounts of Ba were determined by atomic absorption spectrometry on totally oxidized samples, i.e. containing only Ba^{2+}, Fe^{3+}, and O^{2-} ions. The percentage of Fe^{2+} ions in the different samples of magnetite were

TABLE 2

The chemical compositions and mean particle sizes of the samples and their temperatures and enthalpies of oxidation

Amount of Ba in wt.%	Fe^{2+} in % ions [a]	Particle size in nm	Oxidation temperature in °C	ΔH_{ox} in kJ mol^{-1}
0	–	48	170	−86.1
0.29	77	47	185	−81.2
0.44	85	48	189	−83.2
0.56	72	49	195	−83.9
0.73	81	52	208	−85.5
1.06	70	48	188	−80.4
1.49	92	50	190	−82.3
1.74	77	56	211	−84.7
1.77	85	49	213	−81.6
2.09	65	40	219	−84.9
2.46	80	40	247	−83.3

[a] % Fe^{2+} represents the fraction of this ion with respect to that of Fe_3O_4, i.e. 0% corresponds to Fe_2O_3 and 100% to Fe_3O_4.

controlled by chemical complexometry and thermogravimetry. Thus, it is possible to correct the measured enthalpy values. For stoichiometric magnetite sample ($Fe^{2+}/Fe^{3+} = 0.5$), the increase in weight during oxidation is 3.455%. If P_i is the measured increase in weight for a sample i of weight M_i, the corrected enthalpy will be

$$\Delta H_i = \frac{\Delta H_i(\text{measured}) \times 0.03455 M_i}{P_i}$$

This correction is needed because of the high reactivity of these sub-micronic particles, but it is only available for compositions near stoichiometry. Indeed, if the samples have a higher ferric ion content, the energies may be influenced by factors such as diffusion rate changes, chemical heterogeneity, etc.

The chemical composition and the mean particle size of the samples are given in Table 2.

Thermal measurements were made on a Setaram differential scanning calorimeter DSC 111-G with the following analytical conditions: heating rate; $5°C \, min^{-1}$ from ambient to 500°C (oxidation analyses) and from ambient to 830°C (transformation analyses), in an air atmosphere.

OXIDATION OF Fe_3O_4

Oxidation temperature

The variation in the temperature of oxidation of Ba-doped magnetite samples with the barium content is shown in Fig. 3. The gradual increase in the amounts of Ba in the Fe_3O_4 samples leads to a rise in temperature for this exothermal phenomenon from 120°C (Ba-free sample) to 247°C (for 2.47 wt.% of barium).
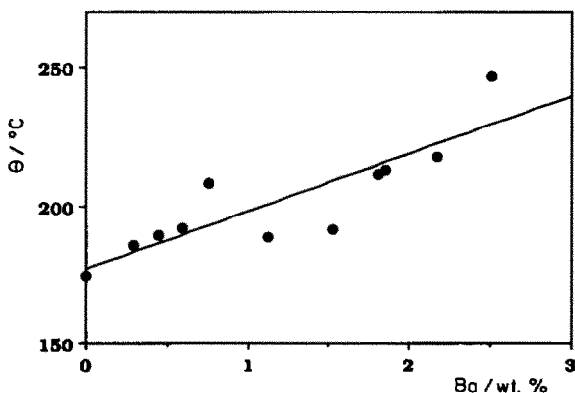

Fig. 3. Variation in the oxidation temperature of Fe_3O_4 with the percentage weight of barium.
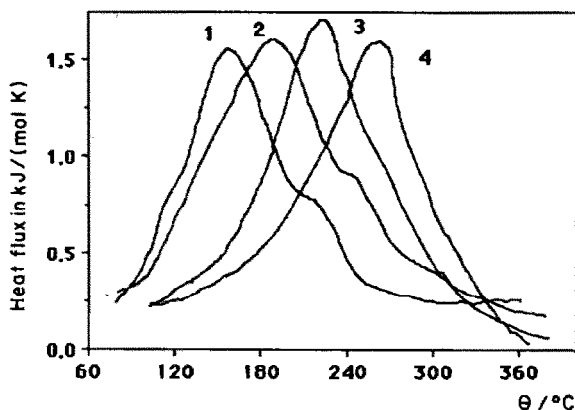
Fig. 4. Thermograms of the microcalorimetric analyses for different Ba contents: sample 1, 0.29 wt.% Ba; sample 2, 0.56 wt.%; sample 3, 1.77 wt.%; sample 4, 2.46 wt.%.

The temperature modifications can be attributed to the barium being located in the surface layers of the particles, where these ions would oppose the migrations of the ferrous ions and electrons towards the solid–gas interface. In this case, the Ba ions represent a diffusion barrier which is particularly difficult to cross when they are numerous at the particle surface. The oxidation process thus needs a higher activation energy, as shown by the shift in the thermal reaction peak.

The displacement is quasi-linear with the increase in Ba, but several points show considerable scatter, greater than the systematic errors of the apparatus and experimental conditions (±2°C).

These gaps result in a deformation of the thermograms, which in some cases leads to reaction peaks with shoulders (Fig. 4), due to a difference in the reactivity of particles in the same sample, which could have three origins

(i) Heterogeneity of Ba doping on the particles, causing oxidation at different temperatures, linked to the amount of Ba in each particle

(ii) Heterogeneity of the particle size distribution, because particle size has an influence on the reaction temperature

(iii) Oxidation at different temperatures for the core and surface of particles, previously shown for Ba-free magnetite samples [18]

Enthalpy of oxidation

The enthalpies of oxidation, as given in Table 2 and on Fig. 5, do not show significant variations. However, previous work [18, 23] has enabled the enthalpy variations to be linked to particles size, i.e. to the distance of migration of the ferrous ions between the bulk (initial position) and the surface (final position). The presence of Ba ions in the superficial layers of
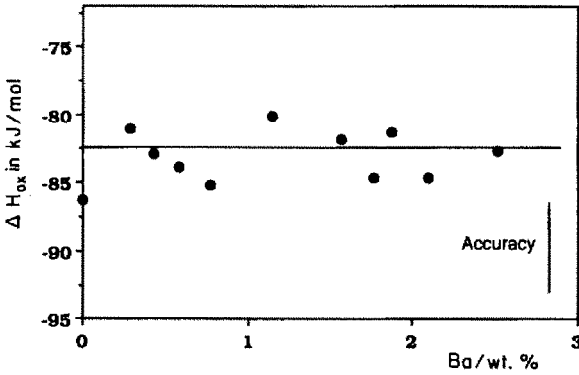
Fig. 5. Variation in the enthalpy of oxidation ΔH_{ox} with the percentage weight of barium.

the particles does not modify the conditions of this migration, because the nature and energy of the bondings in the spinel structure remain identical.

TRANSFORMATION OF γ-Fe$_2$O$_3$

Transformation temperature

The plot of the temperature of the transformation γ-Fe$_2$O$_3 \rightarrow \alpha$-FeO$_3$ versus the amount of Ba (Fig. 6, Table 3) shows two different domains: the first corresponds to a regular increase in the temperature of transformation for Ba contents below about 2 wt.%; above this, the transformation temperature remains constant.

To interpret these results, it is necessary to bear in mind that this transformation corresponds to a lattice rearrangement which takes place by
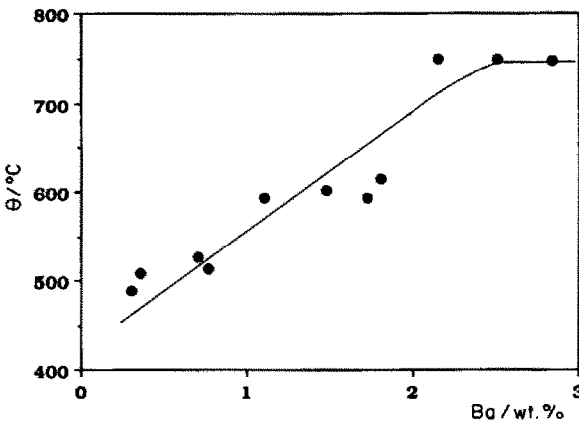

Fig. 6. Temperature of the transformation γ-Fe$_2$O$_3 \rightarrow \alpha$-Fe$_2$O$_3$ as a function of the percentage weight of barium.

TABLE 3

Transformation temperatures and enthalpies of transformation for different amounts of barium

Amount of Ba in wt.%	Transformation temperature in °C	ΔH_{tf} in kJ mol^{-1}
0.29	493	−17.6
0.44	507	−15.8
0.56	–	−14.7
0.73	528	−12.9
1.06	593	−14.5
1.49	605	−11.8
1.77	616	−12.9
2.09	749	−11.0
2.46	751	–
2.85	745	−10.1

relative sliding of the atomic layers which involves the breaking of several Fe–O bonds. However, the study of the spinel structure shows that in the mixed trigonal planes formed from octahedral and tetrahedral sites, the number of bonds to be broken is less than in the kagomé planes, which contain octahedral sites alone. There are in fact four Fe–O bonds for a tetrahedral site and six for an octahedral site.

At the surface of the particles, whatever the textural structure (terraces, ledges, kinks, etc.), the atoms present several unsatisfied bonds. Consequently, the energy needed to generate a dislocation is also minimized here. The addition of a barium ion layer can stabilize the surface layer of the spinel structure, creating bonds with the atoms that have unsatisfied links. In the same way, the doping ions might decrease the number of surface defects, which are potentially favourable sites for the creation and shifting of dislocations.

Thus the gradual increase in the number of Ba ions leads to a rise in temperature linked to the progressive recovering of the surface by a monolayer. When the amount of Ba is greater than 2 wt.%, the surface is saturated, and new ions have no influence on the superficial strain.

In accordance with the particle size, 2 wt.% of Ba corresponds to a monolayer with an atomic density of 5.13 atoms nm^{-2}, i.e. a Ba–Ba distance of 0.44 nm. This distance is the same as that of Ba–Ba in the $BaFe_2O_4$ structure [24], the phase whose presence has been detected on the surface of the particles by IR analysis [22]. When the amount of doping ions is greater than 2 wt.%, new layers are formed without significant influence on the uppermost Fe–O layer. Consequently, the transformation temperature remains the same.
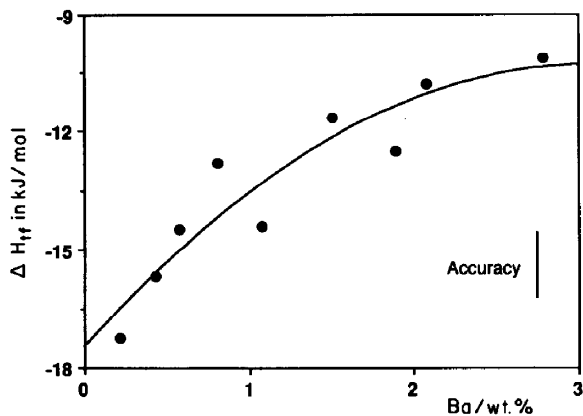
Fig. 7. Variation in the enthalpy of transformation ΔH_{tf} with the percentage weight of Ba.

Enthalpy of transformation

This measurement enables an important modification in the variation of the enthalpy of transformation γ-$Fe_2O_3 \rightarrow \alpha$-$Fe_2O_3$ with the barium content to be detected (Fig. 7, Table 3). Apparently, ΔH_{tf} varies from -17.6 to -10.1 kJ mol^{-1} when the Ba content increases from 0.3 to 2.8 wt.%. It is difficult to explain this very important variation by a chemical or physical process alone. It should be noted that for samples containing large amounts of Ba, the reaction temperature is close to the temperature limit of the apparatus. Thus, it is likely that a part of the reaction peak is not detectable, or is detected but with insufficient accuracy.

Nevertheless, the decrease in ΔH_{tf} could have other origins. Firstly, the formation of barium hexaferrite $BaFe_{12}O_{19}$, which starts at around 500°C, could lead to a decrease in the number of ferric ions capable of reacting to form a corundum structure, because they are stabilized in the more stable hexaferrite structure. Secondly, the baseline used for enthalpy integration could be disturbed by the difference in calorific capacity of the different phases (γ-Fe_2O_3, α-Fe_2O_3, $BaFe_{12}O_{19}$) or by the energy of formation of barium hexaferrite, whose formation spreads over a very wide temperature range. These two possibilities are difficult to confirm due to the lack of literature on this subject. Several empirical rules have been established to link the enthalpy of formation to some physical quantities, but only for binary systems and with insufficient accuracies [25].

CONCLUSIONS

This study by microcalorimetric analysis enables the modifications in the temperature and enthalpies of sub-micronic particles of Ba-doped magnetite to be demonstrated. The presence of this ion in the superficial layers of

the particles plays an important role and we have made the following conclusions.

(i) The temperatures of the two phenomena increase with increasing Ba content due to the presence of a diffusion barrier (for the oxidation $Fe_3O_4 \rightarrow \gamma\text{-}Fe_2O_3$) or to the prevention of the generation and sliding of dislocations (for the transformation $\gamma\text{-}Fe_2O_3 \rightarrow \alpha\text{-}Fe_2O_3$).

(ii) The variation in the enthalpy of oxidation is not modified, because it is linked to the migration of ferrous ions in the spinel structure of the particle core, where Ba ions are not present.

(iii) Finally, the variation of the enthalpy of transformation may be explained by the formation of a new phase, $BaFe_{12}O_{19}$, in the range 500–850°C.

REFERENCES

1 A. Rousset, F. Chassagneux and J. Paris, Mater. Sci., 21 (1986) 3111.
2 B. Gillot, J. Tyranowicz and A. Rousset, Mater. Res. Bull., 10 (1975) 775.
3 B. Gillot, A. Rousset and G. Dupre, J. Solid State Chem., 25 (1978) 263.
4 K.J. Gallagher, W. Feitknecht and U. Mannweiller, Nature, 217 (1968) 1118.
5 P.S. Sidhu, R.J. Gilkes and A.M. Posner, J. Inorg. Nucl. Chem., 39 (1953) 1953.
6 S. Kachi, K. Momiyama and S. Shimizu, J. Phys. Soc. Jpn., 18 (1963) 106.
7 K. Egger and W. Feitknecht, Helv. Chim. Acta, 45 (1962) 2042.
8 U. Colombo, G. Fagherrazzi, F. Gazzarini, G. Lanzavecchia and G. Sironi, Nature, 217 (1968) 1118.
9 Y. Bando, M. Kiyama, T. Takada and S. Kachi, J. Appl. Phys., 4 (1965) 420.
10 G. Dupré, Thesis, Université de Lyon, France, 1976.
11 Y. Imaoka, J. Electron. Soc. Jpn., 36 (1968) 15.
12 A. Rousset, Thesis, Université de Lyon, France, 1969.
13 A. Rousset, J. Paris and P. Mollard, Ann. Chim., 7 (1972) 119.
14 Ch. Sarda, DEA, Université de Toulouse, France, 1986.
15 Ph. Tailhades, Thesis, Université de Toulouse, France, 1988.
16 F.D. Richardson and J.M.E. Jeffes, J. Iron Steel Inst., (1948) 261.
17 M.J.T. Ellingham, J. Soc. Chem. Indust., 63 (1944) 125.
18 Ch. Sarda, F. Mathieu, A.C. Vajpei and A. Rousset, J. Therm. Anal., 32 (1987) 865.
19 A. Ferrier, C. R. Acad. Sci. Paris Ser. C, 264 (1967) 819.
20 H. Imai and M. Senna, J. Appl. Phys., 49(8) (1978) 4433.
21 A. Rousset, G. Boissier, J.P. Caffin and F. Chassagneux, C. R. Acad. Sci. Paris, 299(11) (1984) 781.
22 Ch. Sarda, Ch. Bonino, P. Mollard and A. Rousset, J. Magn. Magn. Mater., 109 (1992) 127.
23 F. Mathieu, Thesis, Université de Toulouse, France, 1990.
24 C. Do-Dinh, E.F. Bertaut and J. Chappert, J. Phys., 30 (1969) 566.
25 O. Kubaschewski and E. Evans, Metallurgical Thermochemistry, 3rd edn., Pergamon Press, Oxford, 1958.